

A β -Ta system for current induced magnetic switching in the absence of external magnetic field

Cite as: AIP Advances **8**, 055918 (2018); <https://doi.org/10.1063/1.5008512>

Submitted: 06 October 2017 • Accepted: 16 November 2017 • Published Online: 03 January 2018

Wenzhe Chen, Lijuan Qian and Gang Xiao

COLLECTIONS

Paper published as part of the special topic on [62nd Annual Conference on Magnetism and Magnetic Materials](#)



View Online



Export Citation



CrossMark

ARTICLES YOU MAY BE INTERESTED IN

[Spin transfer torque devices utilizing the giant spin Hall effect of tungsten](#)

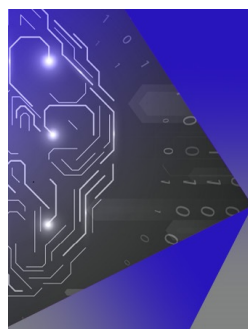
Applied Physics Letters **101**, 122404 (2012); <https://doi.org/10.1063/1.4753947>

[Spin-orbit torque magnetization switching of a three-terminal perpendicular magnetic tunnel junction](#)

Applied Physics Letters **104**, 042406 (2014); <https://doi.org/10.1063/1.4863407>

[Spin Hall effect and current induced magnetic switching in antiferromagnetic IrMn](#)

AIP Advances **8**, 115323 (2018); <https://doi.org/10.1063/1.5059386>



APL Machine Learning

Machine Learning for Applied Physics
Applied Physics for Machine Learning

**First Articles
Now Online!**

A β -Ta system for current induced magnetic switching in the absence of external magnetic field

Wenzhe Chen, Lijuan Qian, and Gang Xiao^a

Department of Physics, Brown University, Providence, Rhode Island 02912, USA

(Presented 9 November 2017; received 6 October 2017; accepted 16 November 2017; published online 3 January 2018)

Magnetic switching via Giant Spin Hall Effect (GSHE) has received great interest for its role in developing future spintronics logic or memory devices. In this work, a new material system (i.e. a transition metal sandwiched between two ferromagnetic layers) with interlayer exchange coupling is introduced to realize the deterministic field-free perpendicular magnetic switching. This system uses β -Ta, as the GSHE agent to generate a spin current and as the interlayer exchange coupling medium to generate an internal field. The critical switching current density at zero field is on the order of 10^6 A/cm² due to the large spin Hall angle of β -Ta. The internal field, along with switching efficiency, depends strongly on the orthogonal magnetization states of two ferromagnetic coupling layers in this system. © 2018 Author(s). All article content, except where otherwise noted, is licensed under a Creative Commons Attribution (CC BY) license (<http://creativecommons.org/licenses/by/4.0/>). <https://doi.org/10.1063/1.5008512>

INTRODUCTION

Spin current, as a result of Giant Spin Hall Effect (GSHE), exerts a spin transfer torque to manipulate the magnetization direction, which provides the possibility of applications in logic and memory devices.¹⁻⁴ Transition metals, such as Hf, Pt, β -Ta and β -W,^{1,3,5-11} possess large spin Hall angles (SHAs); in other words, they are highly efficient in generating a spin current from a charge current. However, there exists a major obstacle: an external field is required to switch the perpendicular magnetization deterministically. This obstacle makes GSHE devices technologically complicated and energy-consuming. Therefore, realizing zero-field deterministic perpendicular magnetic switching has recently been a popular topic in the spintronics research and development communities. Some researchers have tried to introduce a so-called lateral structure asymmetry,¹² but this is very difficult to implement in practice. Others have attempted to replace the transition metals with the antiferromagnetic (AFM) materials to generate spin current and spin transfer torque.¹³⁻¹⁷ With the help of AFM material, the internal exchange biasing field exerted on the adjacent perpendicular Ferromagnetic (FM) layer makes field-free magnetic switching possible. However, this kind of approach might lead to two issues: an incomplete field-free magnetic switching,¹⁷ and a too-large critical switching current density due to the small SHAs of AFM materials.¹⁸

In this article, we introduce a GSHE material system with the structure of FM/NM/FM. This sandwich structure has been successfully utilized in Giant Magnetoresistance (GMR)^{19,20} and Magnetic Tunneling Junction (MTJ).^{21,22} We use β -Ta, which has a high spin Hall angle, as the non-magnetic (NM) material. Other non-magnetic transition metals may also be used as NM in this material system FM/NM/FM. Through the NM layer, the exchange coupling effect between two FM layers generates the internal field to realize field-free switching. The critical switching current density is on the order of 10^6 A/cm² (1 MA/cm²). Finally, we also study the samples with different β -Ta thickness and annealing conditions in order to understand the field-free switching mechanism better.

^aGang_Xiao@brown.edu

SAMPLE PREPARATION AND CHARACTERIZATION

We used a magnetron sputtering system to deposit the samples on thermally oxidized silicon wafers under the base pressure of 2×10^{-8} Torr. Figure 1(a) is a cross-section view of our sample structure from bottom to top sequenced as: Si/SiO₂/Ta(4.0)/CoFeB(3.0)/ β -Ta(x)/CoFeB(1.0)/MgO(1.6)/Ta(1.0), (the number in the parentheses represents the thickness of the corresponding layer with the unit of nanometer). The β -Ta layer's thickness x varies from 1.2 nm to 4.8 nm. In this article, x equals 2.4 nm if not specified. The bottom 4 nm-thick Ta layer acts as the seeding layer to facilitate the sample growth. The 3 nm-thick CoFeB layer gives in-plane magnetization. With the help of the MgO layer, the 1 nm-thick CoFeB layer possesses perpendicular magnetization anisotropy (PMA). The top 1 nm-thick Ta layer protects the whole stack from oxidation. For electric measurement, we patterned our samples into $20 \mu\text{m} \times 55 \mu\text{m}$ standard Hall bars through photolithography and ion milling. Finally, we annealed our samples at 150°C for 1 hour under an external magnetic field of ~ 0.42 T in a vacuum chamber of 2×10^{-6} Torr. Using parallel resistance rule, we estimate the resistivity of Ta layer to be $210.1 \mu\Omega\text{-cm}$ to $200.5 \mu\Omega\text{-cm}$ for samples with x from 1.2 to 4.8 nm. Comparing with the typical resistivity of α -Ta and β -Ta,²³ we are confident about the achievement of β -phase in Ta solid.

Figure 1(b) shows the sandwich structure CoFeB(\rightarrow)/ β -Ta/CoFeB(\uparrow) and its Hall measurement schematic using the illustrated Cartesian coordinate system (x - y - z). The key point in our sample is the orthogonal magnetization (shown with red arrows) of the two CoFeB layers. We confirm this orthogonal magnetization states using the following methods. Figure 1(c) shows the Hall resistance with a z -axis magnetic field. The anomalous Hall resistance²⁴ is given by $\rho_{xy} = R_0 H_Z + R_S M_z$, so the higher/lower Hall resistance refers to up/down magnetization state. The perfect square loop in Figure 1(c) exhibits the robust PMA in the top 1 nm-thick CoFeB layer. The coercive field is 1.25 ± 0.09 mT. Interestingly, the existence of PMA does not depend on the external field direction during the annealing process; in other words, both perpendicular and in-plane annealed samples

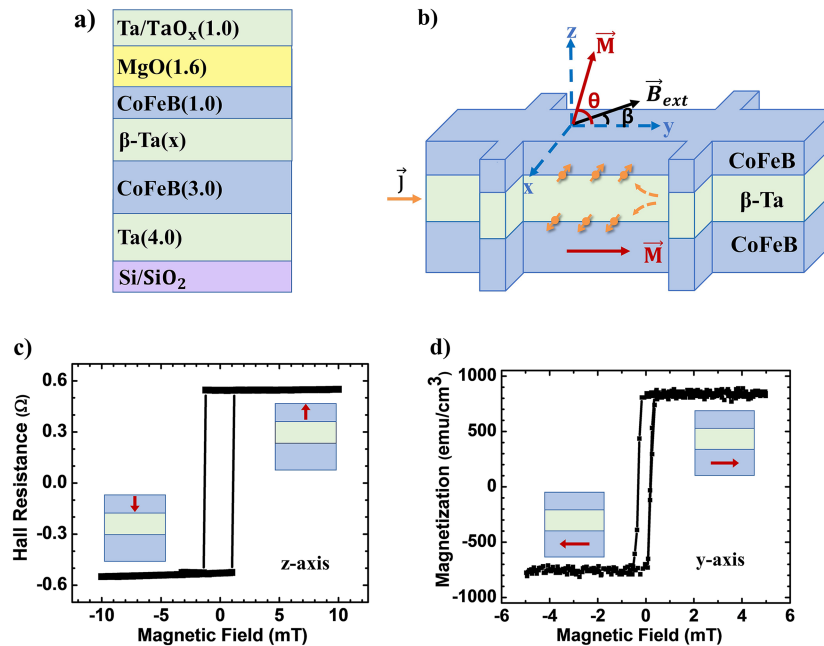


FIG. 1. Structure and characterization of a multilayer sample, Si/SiO₂/Ta(4.0)/CoFeB(3.0)/ β -Ta(x)/CoFeB(1.0)/MgO(1.6)/Ta(1.0). a) Cross-section view of the multilayer sample. The number in the parentheses represents the thickness of the corresponding layer with the unit of nanometer. b) Schematic of Hall measurement. The spin current, coming from charge current \vec{J} through the β -Ta layer, accumulates at the CoFeB/Ta and Ta/CoFeB interfaces. θ is the angle between the top layer's magnetization \vec{M} and the y -axis; and β is a small angle (about $1^\circ \sim 2^\circ$) in the y - z plane between the external magnetic field \vec{B}_{ext} and the y -axis. c) Anomalous Hall measurement with perpendicular (z -axis) magnetic field. The high/low Hall resistance refers to the up/down magnetization state (red arrow) of the top CoFeB layer. d) Magnetization hysteresis loops within the magnetic field of 5.0 mT along the y -axis.

possess the robust PMA. In this article, our samples are annealed under an in-plane field unless specified. We used Vibrating Sample Magnetometer (VSM) to characterize the magnetization of the 3 nm-thick CoFeB layer. The magnetic hysteresis loop in Figure 1(d) exhibits a perfect square shape. The contribution from 1 nm-thick CoFeB layer with PMA is negligible, since its anisotropy field is hundreds of mT.⁵ The easy axis of the 3 nm-thick CoFeB layer is along the y-axis and the coercive field H_c is about 0.2~0.3 mT.

PULSE CURRENT INDUCED MAGNETIC SWITCHING

Magnetic switching is the result of competition among three collinear torques:^{5,7,25} spin transfer torque $\vec{\tau}_{st}$ from the spin current; external torque $\vec{\tau}_{ext}$ from the external magnetic field B_{ext} ; anisotropy torque $\vec{\tau}_{an}$ from the magnetic anisotropy B_{an}^0 . The torque projected on the x-axis is as follows:

$$\tau_{TOT} = \vec{x} \cdot (\vec{\tau}_{st} + \vec{\tau}_{ext} + \vec{\tau}_{an}) = \tau_{ST}^0 + B_{ext} \sin(\theta - \beta) - B_{an}^0 \sin\theta \cos\theta$$

When the spin transfer torque is large enough, it switches the magnetization of the 1 nm-thick CoFeB layer to a new and stable lower-energy state. This switchings between up/down magnetization states of 1 nm-thick CoFeB layer require an external field B_{ext} to break the mirror symmetry with respect to the x-z plane.^{7,12}

We have conducted the pulse current induced magnetic switching under an external magnetic field from ± 8.0 mT to ± 0.0 mT. The magnetic field is calibrated carefully and its error is smaller than

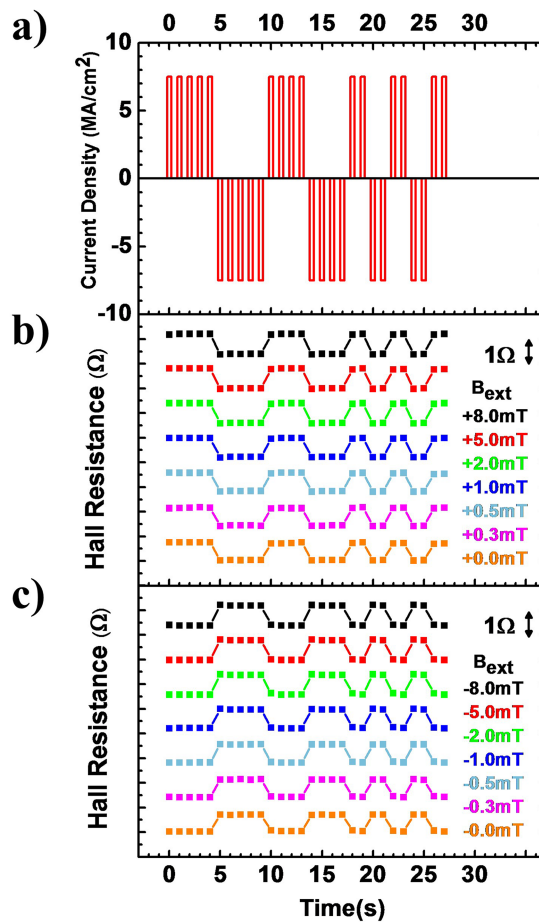


FIG. 2. Pulse current induced magnetic switching. a) Pulse current pattern with time. The magnitude of both positive and negative pulse currents is 7.5×10^6 A/cm² and the pulse width is 0.2 ms. b) c) Hall resistance response under the pulse current sequence in Figure 2(a) under an external magnetic field from ± 8.0 mT to ± 0.0 mT.

0.3 Oe. Figure 2(a) shows a time sequence of bipolar current pulses with the width of 0.2 ms and the amplitude of 7.5 MA/cm². Figures 2(b) and 2(c) show that the up/down magnetization state is controlled by the pulse current under the different external field. In Figure 2(b), positive current pulses can switch the magnetization from the down state to the up state, and vice versa. The measurement in Figure 2(c) is similar to that in Figure 2(b), except under a negative external field. The negative external field leads to the opposite switching behavior, i.e., the down state can be switched to up state by negative current pulses. In Figures 2(b) and 2(c), deterministic magnetic switching at 0 mT is clearly observed. It is “ferromagnetic” interlayer exchange coupling of CoFeB/ β -Ta/CoFeB that plays an important role in generating internal field to switch magnetization at 0 mT. Consequently, the up/down magnetization state is deterministically switched by a train of bipolar current pulses under the internal or external field.

The widely-investigated interlayer exchange coupling^{26–29} exists in all 3d, 4d and 5d transition metals in the structure of FM/NM/FM.²⁷ The exchange coupling effect^{28,29} is related to the topological property of the Fermi surface of transition metal, leading to oscillation in polarity (such as FM and AFM coupling). In our structure CoFeB(\rightarrow)/ β -Ta/CoFeB(\uparrow), through the β -Ta NM layer, the 3 nm-thick CoFeB FM layer’s in-plane magnetization couples with the 1 nm-thick CoFeB FM layer’s perpendicular magnetization. Visually, the 1 nm-thick CoFeB layer’s magnetization tilts slightly away from the perpendicular (z-axis) direction (Figures 1(a) and 1(b)). This is equivalent to an internal field to break the x-z plane’s mirror symmetry.¹²

In our samples, exchange coupling effect works in a large β -Ta thickness range varying from 1.2 nm to 4.8 nm. In this range, the coupling is always ferromagnetic. The interlayer exchange coupling about β -Ta has not been studied in the literature, although some data of α -Ta is available.²⁷ While α -Ta is bcc structure with the low resistivity of 24~50 $\mu\Omega$ -cm, β -Ta is tetragonal structure with the high resistivity of 180~220 $\mu\Omega$ -cm.²³ In Co/ α -Ta/Co and Fe/ α -Ta/Fe,²⁷ no oscillating behavior is observed and the exchange coupling strength is ~ 0.01 erg/cm². We roughly estimate the internal field from interlayer exchange coupling to be a couple of Oe. For numerical analysis, the interlayer exchange coupling strength is estimated as only ~ 0.001 erg/cm² at 2.4 nm β -Ta sample.

INFLUENCE OF β -Ta THICKNESS AND ANNEALING CONDITION ON SWITCHING EFFICIENCY

We have studied the different β -Ta thickness x and its effect in switching. Figure 3(a) summarizes the switching efficiency versus the β -Ta thickness. Switching efficiency is given by $\Delta R_{0mT}/\Delta R_{8mT}$, where ΔR_{0mT} and ΔR_{8mT} are the average high/low Hall resistance difference during switching at 0.0 mT and 8.0 mT, respectively. The switching efficiency is a result of competition between the SHA of β -Ta and the internal field from interlayer exchange coupling effect. Exchange coupling strength is theoretically predicted to decay rapidly with an increasing NM layer’s thickness.^{28,29} According to studies in the GSHE systems, the SHA of transition metal is positively correlated with its thickness.⁸ In Figure 3(d), the optimal switching efficiency is as high as 88.5% occurring at the β -Ta thickness of 2.4 nm. The switching efficiency is only 30% when β -Ta thickness is 1.2 nm. When β -Ta thickness x is larger than 1.8 nm, the switching efficiency is generally stable and larger than 80% except for $x=3.6$ nm.

Finally, we have also studied the relationship between switching efficiency and magnetic annealing condition. For a control experiment, we prepare the perpendicular annealed samples, i.e., samples annealed at 150 °C for 1 hour under the z-axis (perpendicular) magnetic field of ~ 0.42 T. As mentioned before, the 1 nm-thick CoFeB layers of the perpendicular annealed samples also show the robust PMA. However, the 3 nm-thick CoFeB layer with in-plane magnetization exhibits the multidomain state, shown in the y-axis magnetization hysteresis loops of Figure 3(b). For the perpendicular annealed sample, its remnant magnetization is only about 65% of the saturated magnetization. Figure 3(c) shows its magnetic switching induced by the same pulse current sequence as in Figure 2(a) under an external field from 8.0 mT to 0.0 mT. The magnetic switching of the in-plane annealed sample in Figure 2(b) outperforms the perpendicular annealed sample in Figure 3(c). It is noteworthy that the magnetic switching is incomplete at 0.0 mT. Figure 3(d) displays the high/low Hall resistance difference ratio $\Delta R_{B_{ext}}/\Delta R_{8mT}$ versus external fields B_{ext} . When B_{ext} is larger than

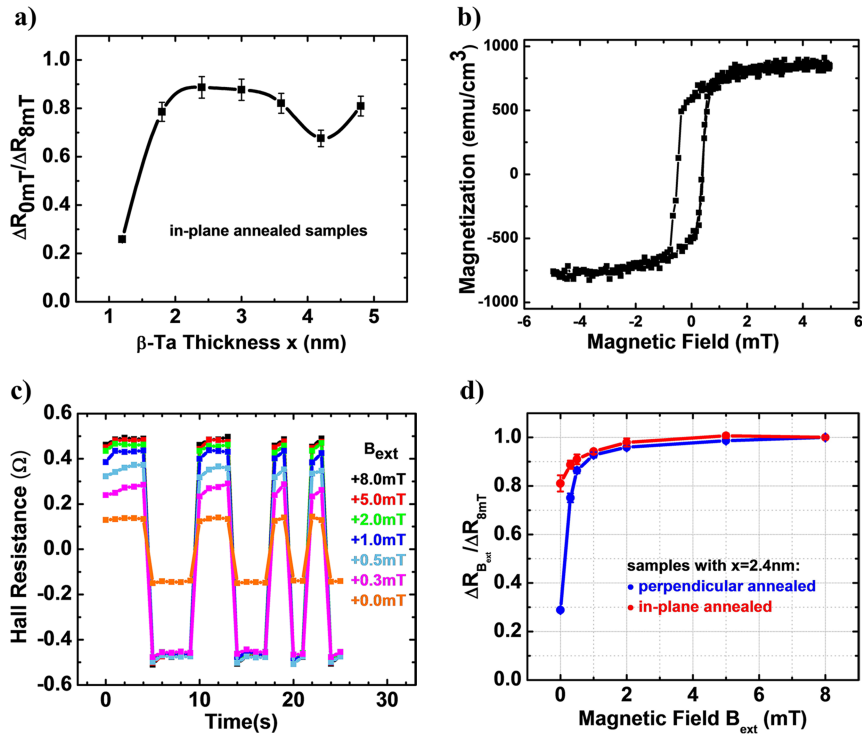


FIG. 3. Switching efficiency with different β -Ta thicknesses and annealing conditions. a) Switching efficiency $\Delta R_{0mT}/\Delta R_{8mT}$ versus the β -Ta thickness. All the samples are annealed under in-plane field. b) Magnetization hysteresis loop of the perpendicular annealed sample. c) Hall resistance response of the perpendicular annealed samples under the pulse current sequence in Figure 2(a) under an external field from 8.0 mT to 0.0 mT. d) High/low Hall resistance difference ratio $\Delta R_{B_{ext}}/\Delta R_{8mT}$ versus the external magnetic field B_{ext} . The β -Ta thickness of both samples is 2.4 nm. The blue curve is the perpendicular annealed sample and the red curve is the in-plane annealed sample.

1.0 mT, the switching efficiency $\Delta R_{B_{ext}}/\Delta R_{8mT}$ of the in-plane and perpendicular annealed samples do not differ significantly (less than 2%), since external field still dominates magnetic switching behaviors. When B_{ext} is smaller than 1.0 mT, the external field becomes so weak that the magnetic switching relies partially, or even mainly, on the internal field from exchange coupling effect. For the perpendicular annealed samples, the internal field is weakened by the multi-domain state of the 3 nm-thick CoFeB layer. In the absence of the external field, the switching efficiency $\Delta R_{0mT}/\Delta R_{8mT}$ of the in-plane annealed sample is as high as 80%, while the perpendicular annealed sample is only 30%. This result is consistent with the different domain states of the in-plane magnetizations in Figures 1(d) and 3(b). Through controlling for the 3 nm-thick CoFeB layer's in-plane magnetization, we can conclude that the interlayer exchange coupling effect of CoFeB(\rightarrow)/ β -Ta/CoFeB(\uparrow) with orthogonal magnetization plays an important role in field-free deterministic magnetic switching.

CONCLUSION

In this work, we develop a new approach with the indirect exchange coupling effect to realize the deterministic field-free current induced magnetic switching. We use β -Ta, with large spin Hall angle, both as a GSHE solid to generate the spin current and as a conducting medium to generate exchange coupling as a replacement for an external magnetic field. We have achieved deterministic and reliable field-free switching, as well as the low critical switching current density of $6\sim 7$ MA/cm² at 0.0 mT. We also study the switching efficiency with different β -Ta thicknesses and different annealing conditions. The optimal switching efficiency, as high as 88.5%, is achieved at the β -Ta thickness of 0.24 nm. Using the control experiments, we confirm that the internal field, arising from the exchange coupling effect of CoFeB/ β -Ta/CoFeB, is responsible for magnetic switching in the absence of the external field.

ACKNOWLEDGMENTS

This work was supported by National Science Foundation through Grants No. DMR-1307056 and by Nanoelectronics Research Initiative (NRI) through the Institute for Nanoelectronics Discovery and Exploration (INDEX).

- ¹ J. Sinova, S. O. Valenzuela, J. Wunderlich, C. H. Back, and T. Jungwirth, "Spin Hall effects," *Reviews of Modern Physics* **87**, 1213–1260 (2015).
- ² J. Hirsch, "Spin Hall effect," *Physical Review Letters* **83**, 1834–1837 (1999).
- ³ L. Liu *et al.*, "Spin-torque switching with the giant spin Hall effect of tantalum," *Science* **336**, 555–558 (2012).
- ⁴ I. M. Miron *et al.*, "Perpendicular switching of a single ferromagnetic layer induced by in-plane current injection," *Nature* **476**, 189–193 (2011).
- ⁵ Q. Hao and G. Xiao, "Giant spin Hall effect and magnetotransport in a Ta/CoFeB/MgO layered structure: A temperature dependence study," *Physical Review B* **91** (2015).
- ⁶ Q. Hao, W. Chen, and G. Xiao, "Beta (β) tungsten thin films: Structure, electron transport, and giant spin Hall effect," *Applied Physics Letters* **106**, 182403 (2015).
- ⁷ L. Liu, O. Lee, T. Gudmundsen, D. Ralph, and R. Buhrman, "Current-induced switching of perpendicularly magnetized magnetic layers using spin torque from the spin Hall effect," *Physical Review Letters* **109**, 096602 (2012).
- ⁸ Q. Hao and G. Xiao, "Giant spin Hall effect and switching induced by spin-transfer torque in a W/Co 40 Fe 40 B 20/MgO structure with perpendicular magnetic anisotropy," *Physical Review Applied* **3**, 034009 (2015).
- ⁹ C.-F. Pai *et al.*, "Spin transfer torque devices utilizing the giant spin Hall effect of tungsten," *Applied Physics Letters* **101**, 122404 (2012).
- ¹⁰ C.-F. Pai *et al.*, "Enhancement of perpendicular magnetic anisotropy and transmission of spin-Hall-effect-induced spin currents by a Hf spacer layer in W/Hf/CoFeB/MgO layer structures," *Applied Physics Letters* **104**, 082407 (2014).
- ¹¹ Y. Wang, P. Deorani, X. Qiu, J. H. Kwon, and H. Yang, "Determination of intrinsic spin Hall angle in Pt," *Applied Physics Letters* **105**, 152412 (2014).
- ¹² G. Yu *et al.*, "Switching of perpendicular magnetization by spin-orbit torques in the absence of external magnetic fields," *Nat Nanotechnol* **9**, 548–554 (2014).
- ¹³ W. J. Kong *et al.*, "Field-free spin Hall effect driven magnetization switching in Pd/Co/IrMn exchange coupling system," *Applied Physics Letters* **109**, 132402 (2016).
- ¹⁴ Y.-C. Lau, D. Betto, K. Rode, J. M. D. Coey, and P. Stamenov, "Spin-orbit torque switching without an external field using interlayer exchange coupling," *Nat Nano* **11**, 758–762 (2016).
- ¹⁵ Y. W. Oh *et al.*, "Field-free switching of perpendicular magnetization through spin-orbit torque in antiferromagnet/ferromagnet/oxide structures," *Nat Nanotechnol* **11**, 878–884 (2016).
- ¹⁶ S. Fukami, C. Zhang, S. DuttaGupta, A. Kurenkov, and H. Ohno, "Magnetization switching by spin-orbit torque in an antiferromagnet-ferromagnet bilayer system," *Nat Mater* **15**, 535–541 (2016).
- ¹⁷ A. van den Brink *et al.*, "Field-free magnetization reversal by spin-Hall effect and exchange bias," *Nat Commun* **7**, 10854 (2016).
- ¹⁸ W. Zhang *et al.*, "Spin Hall effects in metallic antiferromagnets," *Phys Rev Lett* **113**, 196602 (2014).
- ¹⁹ M. N. Baibich *et al.*, "Giant magnetoresistance of (001)Fe/(001)Cr magnetic superlattices," *Physical Review Letters* **61**, 2472–2475 (1988).
- ²⁰ C. Reig, M.-D. Cubells-Beltrán, and D. Ramírez Muñoz, "Magnetic field sensors based on giant magnetoresistance (GMR) technology: Applications in electrical current sensing," *Sensors* **9**, 7919–7942 (2009).
- ²¹ X. Liu, W. Zhang, M. J. Carter, and G. Xiao, "Ferromagnetic resonance and damping properties of CoFeB thin films as free layers in MgO-based magnetic tunnel junctions," *Journal of Applied Physics* **110**, 033910 (2011).
- ²² J. Hayakawa, S. Ikeda, F. Matsukura, H. Takahashi, and H. Ohno, "Dependence of giant tunnel magnetoresistance of sputtered CoFeB/MgO/CoFeB magnetic tunnel junctions on MgO barrier thickness and annealing temperature," *Japanese Journal of Applied Physics* **44**, L587 (2005).
- ²³ M. H. Read and C. Altman, "A new structure in tantalum thin films," *Applied Physics Letters* **7**, 51–52 (1965).
- ²⁴ N. Nagaosa, J. Sinova, S. Onoda, A. MacDonald, and N. Ong, "Anomalous Hall effect," *Reviews of Modern Physics* **82**, 1539–1592 (2010).
- ²⁵ P. M. Haney, H.-W. Lee, K.-J. Lee, A. Manchon, and M. D. Stiles, "Current induced torques and interfacial spin-orbit coupling: Semiclassical modeling," *Physical Review B* **87** (2013).
- ²⁶ S. Parkin, N. More, and K. Roche, "Oscillations in exchange coupling and magnetoresistance in metallic superlattice structures: Co/Ru, Co/Cr, and Fe/Cr," *Physical Review Letters* **64**, 2304 (1990).
- ²⁷ S. S. Parkin, "Systematic variation of the strength and oscillation period of indirect magnetic exchange coupling through the 3d, 4d, and 5d transition metals," *Phys Rev Lett* **67**, 3598–3601 (1991).
- ²⁸ P. Bruno and C. Chappert, "Oscillatory coupling between ferromagnetic layers separated by a nonmagnetic metal spacer," *Phys Rev Lett* **67**, 1602–1605 (1991).
- ²⁹ P. Bruno and C. Chappert, "Ruderman-Kittel theory of oscillatory interlayer exchange coupling," *Physical Review B* **46**, 261–270 (1992).